J Intell Robot Syst (2013) 69:347–360
DOI 10.1007/s10846-012-9765-7

Standoff Target Tracking using a Vector Field for Multiple Unmanned Aircrafts

Seunghan Lim · Yeongju Kim · Dongjin Lee · Hyochoong Bang

Received: 22 June 2012 / Accepted: 10 July 2012 / Published online: 6 September 2012

Abstract This paper presents strategies for standoff target tracking by a team of unmanned aircrafts using vector field. Many methods to the vector field approach were investigated in other papers, but a modified vector field is introduced to obtain new interesting characteristics in this paper. The modified vector field satisfies more constraints. We introduce two guidance modes to track a target: one is a capturing mode and the other one is a loitering mode. In the capturing mode, aircrafts can arrive at desired positions and time, i.e., unmanned aircrafts can capture a target simultaneously from all sides. After a target is captured, the guidance mode is changed to the loitering mode. Then the relative spacing among aircrafts is controlled by a standoff distance command and a speed command. Hence, they track a target with a desired formation.

S. Lim (✉) · Y. Kim · D. Lee · H. Bang
Division of Aerospace Engineering,
School of Mechanical, Aerospace and Systems Engineering, KAIST, Daejeon, South Korea
e-mail: shlim@ascl.kaist.ac.kr

Y. Kim
e-mail: yjkim@ascl.kaist.ac.kr

D. Lee
e-mail: djlee@ascl.kaist.ac.kr

H. Bang
e-mail: hcbang@ascl.kaist.ac.kr

Keywords UAV · Vector field guidance · Vector field control · Vector field · Target tracking · Cooperative control

1 Introduction

Unmanned aircrafts (UAs) must navigate autonomously to accomplish missions. The convectional navigation procedure consists of path planning, path following, and attitude control. It is of great importance that an UA have the capability to plan paths and follow them precisely. The most fundamental path planning is connecting waypoints sequentially. For target tracking problems, a circular path around the target is the most popular.

After a path is designed, there are two approaches in following problem. The first approach is referred to as trajectory tracking [1]. This makes a vehicle follow a reference point. The vehicle travels along the path with a predefined velocity. This approach requires the vehicle to be in a certain position at a certain time, which can cause problems for small UAs with disturbances such as strong wind, and thus such UAs cannot satisfy the requirements. The second approach is a path following approach [2]. The objective of path following is for the vehicle to be on the path, and placing vehicles at a certain time is not considered. The potential field approach and the vector field

approach are popular path following algorithms in robotics [3–5]. In the potential field approach, the direction where the vehicle should go is defined on the basis of a charge field, where obstacles are considered as charges with a repelling force and the goal position is considered as a charge with an attractive force. The most notable weakness of this method is a local minima problem for a collision avoidance issue [6, 7]. The local minima are the basis points of attraction where the vehicle can be trapped. A vector field is constructed by representing a desired course and desired ground speed. When a current position and a desired path are given, the vector field is essentially painted on the ground around the desired path. Thus, the desired course and ground speed is represented by a function of the current position. Some researchers used the desired heading and desired airspeed instead of the course and ground speed.

Surveillance or target tracking is a popular and important mission. In a standoff target tracking problem, there are two main approaches. The first is the stability-oriented approach, in which control laws are designed to produce asymptotic stability to desired reference states. The second is the behavior-oriented approach, in which the motion onto the reference state is also part of the design process. The stability-oriented method includes path tracking approaches in which a standoff loitering path is defined, and a virtual target on the path is specified to be tracked by UAs [8, 9]. A control law is designed to regulate the lateral and heading error to zero by calculating an intercept course that varies with the lateral distance. In this approach, local stability can be achieved, but it is more complicated to achieve global behavior because the computed virtual target on the path is not unique.

The behavior-oriented approach explicitly specifies the motion behavior toward a desired path, and this approach requires a controller to accomplish this motion. A vector field is constructed to provide the motion, such as the desired course and speed of the UAs at any position in the domain. This approach comes from the potential field approach studied in mobile robotics [10, 11], and consists of sink and circulation behavior to and around the origin, respectively. Frew et al. used this approach, and they added compensation and coordination terms for the wind and multiple vehicles, respectively. They used the idea from Lawrence et al.'s paper [12, 13]. They proposed a globally stable control law for relative spacing on a loitering circle. They also guaranteed a standoff distance from the moving target while satisfying an airspeed constraint.

We extended our research from Frew et al.'s work to achieve simultaneous capture and to improve performance. The remainder of this paper is presented as follows. In Section 2, we model the kinematics of the UA before defining a vector field. The course and ground speed are considered as guidance commands. In Section 3, the modified vector field is introduced for standoff target tracking, and some interesting results are shown. The guidance mode is divided into the capturing mode and the loitering mode. In the capturing mode, the vector field guides the UAs to arrive at the desired position and time to capture a target simultaneously from all sides. In the loitering mode, it controls the relative spacing among the UAs. In Section 4, strategies to implement a standoff target tracking problem are introduced, and some simulation results are shown. Conclusions are in Section 5 with a brief mention of future investigations.

2 Problem Statement

A flight control system (FCS) must be equipped to control UAs, and it has a hierarchical command structure. In this paper, it is assumed that a FCS has two layers; a guidance layer and a control layer. They are a higher and a lower level controller, respectively. The guidance layer generates the ground speed, the course over ground, and the altitude command. Then, the control layer controls actuators to track the guidance commands. This paper focuses only on the guidance layer and this layer is designed based on a point-mass model on a two dimensional plane. And an altitude command is assumed as constant.

A kinematic model of an UA in wind is

$$\begin{aligned} \dot{x} &= s_a \cdot \cos\psi + W_x \\ \dot{y} &= s_a \cdot \sin\psi + W_y \end{aligned} \tag{1}$$

where $[x, y]^{\mathrm{T}} \in \Re^2$ is the inertial position of the UA, s_a is the air speed, $\psi \in [0,2\pi)$ is the yaw angle, ψ_d is the desired yaw angle, and $[W_x, W_y]^{\mathrm{T}}$ is the inertial velocity of the wind. Frew et al. assumed that the wind speed was slow, constant, and known [12]. When we have the desired course and ground speed, the yaw angle and the airspeed can be derived from them by considering the wind velocity. In fact, measuring the wind velocity requires an air data system and a GPS receiver, and an air data system is more expensive than a GPS receiver. A GPS receiver measures not only the inertial position (actually a position on the Earth-fixed coordinates), but also the ground speed and course accurately; otherwise an air data system measures relative airspeed only. Therefore, we assume that the lower level controller can track the course and the ground speed well as Griffiths et al. and Nelson et al. did [14, 15]. And it is reasonable when the wind is not very strong.

Hence, a first-order time-delayed system with the course and ground speed is used, and it consists of a motion of target and a relative motion with regard to a target as below.

$$\begin{aligned} \dot{x} &= s \cdot \cos\chi = \dot{x}_r + \dot{x}_t \\ \dot{y} &= s \cdot \sin\chi = \dot{y}_r + \dot{y}_t \\ \dot{s} &= \tau_s (s - s_d) \\ \dot{\chi} &= \tau_\chi \langle \chi - \chi_d \rangle \end{aligned} \tag{2}$$

where s is the ground speed, s_d *is the desired speed*, χ is the course, χ_d *is the desired course*, $[x_t, y_t]^{\mathrm{T}}$ *is the target position on the inertial frame, and* $[x_r, y_r]^{\mathrm{T}}$ is the relative position from the target. τ_s and τ_χ are time constants of the first-order kinematics of the speed and course, respectively. The geometry relationship is shown in Fig. 1.

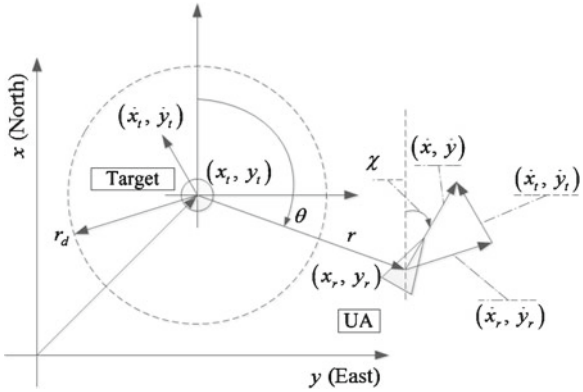

Fig. 1 Geometry relationship

3 Vector Field for Standoff Target Tracking

The desired relative motion for standoff target tracking was generated based on the Lyapunov vector field. It was opened to the public and was used by various researchers [12–19]. The vector field introduced in this paper is modified from them. The desired motion is the relative motion with regard to the target; therefore, the vector field is defined in a relative frame as

$$\begin{bmatrix} \dot{r} \\ r\dot{\theta} \end{bmatrix} = \frac{s_r}{\sqrt{r^4 + \left(p^2 - 2\right) r_d^2 r^2 + r_d^4}} \begin{bmatrix} -\left(r^2 - r_d^2\right) \\ p \cdot r_d \cdot r \end{bmatrix} \tag{3}$$

where $r = \mathrm{sqrt}\left(x_r^2 + y_r^2\right)$, $\theta = \mathrm{atan2}(y_r, x_r)$, s_r is the desired relative speed, r_d is the desired standoff distance from the target, and p is a non-dimensional parameter to transfigure the vector field. If p is two, then Eq. 3 is same as the proposed Lyapunov vector field from [12]. Due to the variable p, new interesting characteristics are derived, and consequently capturing the target simultaneously from all sides becomes feasible. The magnitude of the vector is the same as s_r, since the scalar value on the right hand side normalizes the vector. Examples of the modified vector field are shown in Fig. 2. The magnitude of p in the left figure is smaller than the one in the right, and it is positive and negative in the left and the right figures, respectively.

The course change rate or the curvature of a path is significant, since they are directly correlated to the turning rate of the UAs. A field designer must consider limitations of dynamics; therefore, analyzing the curvature is necessary. If the target is stationary, the course is

$$\chi_0 = \mathrm{atan2}(\dot{y}, \dot{x}) = \mathrm{atan2}(\dot{y}_r, \dot{x}_r) \tag{4}$$

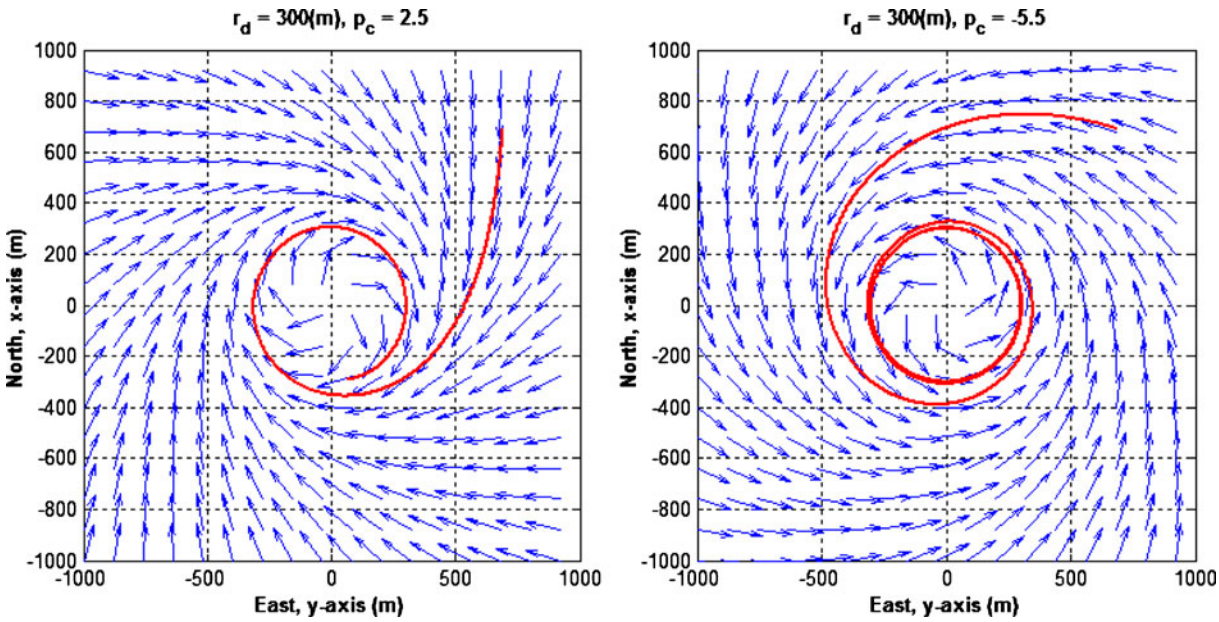

Fig. 2 Examples of the modified Vector Field. The *left* figure is constructed by positive and smaller magnitude p, and the *right* figure is constructed by negative and larger magnitude p

where the subscript 0 implies that the target is stationary. Then, the derivative of the course with respect to time is

$$\dot{\chi}_0 = \frac{s_r \cdot p \cdot r_d^3 \left\{\left(p^2-2\right) r^2 + 2r_d^2\right\}}{\left\{r^4 + \left(p^2-2\right) r_d^2 \cdot r^2 + r_d^4\right\}^{3/2}}. \tag{5}$$

Hence, the curvature of this field when the target is stationary is expressed as

$$\kappa_0 (r) = \frac{\dot{\chi}_0}{s_r} = \frac{p \cdot r_d^3 \left\{\left(p^2-2\right) r^2 + 2r_d^2\right\}}{\left\{r^4 + \left(p^2-2\right) r_d^2 \cdot r^2 + r_d^4\right\}^{3/2}}, \tag{6}$$

and the results are shown in Fig. 3. The maximum curvature deserves a little consideration, since the UAs might be operated in the region of or outside of r_d. That is, the curvature only near r_d is worthwhile to consider, since the curvature is monotonically decreased when r is increased and larger than r_d.

The stability of this field can be shown easily using a Lyapunov function. Consider a Lyapunov function as

$$\mathrm{V}_r = \frac{1}{2}\left(r^2 - r_d^2\right)^2. \tag{7}$$

Then the derivative of the Lyapunov function V_r with respect to time is

$$\frac{\mathrm{dV}_r}{\mathrm{dt}} = \frac{-2s_r \cdot r\left(r^2 - r_d^2\right)^2}{\sqrt{\left(r^2 - r_d^2\right)^2 + \left(p \cdot r_d \cdot r\right)^2}}. \tag{8}$$

As you can see above, it is negative semi-definite, i.e., the field always converges to the loitering circle except for when $r = 0$ or r_d.

3.1 Control of Arrival Position and Time

When the position of the target after t_{ren} is known or can be estimated, a loitering circle at that time is also determined, where t_{ren} is the remaining time of arrival. From Eq. 3, the estimated time of arrival from r_c to r_f, t_{eta}, can be computed numerically. r_c and r_f are the current distance and desired final distance from the target, respectively, and s_c is the current ground speed of the UA.

$$t_{\mathrm{eta}} = \int_{r_c}^{r_f} \left[-\frac{1}{s_c}\sqrt{1 + \left(\frac{p \cdot r_d \cdot r}{r^2 - r_d^2}\right)^2}\right] \mathrm{d}\, r \tag{9}$$

where r_c and r_f are assumed as $r_c > r_f > r_d > 0$. Solving the definite integration analytically is

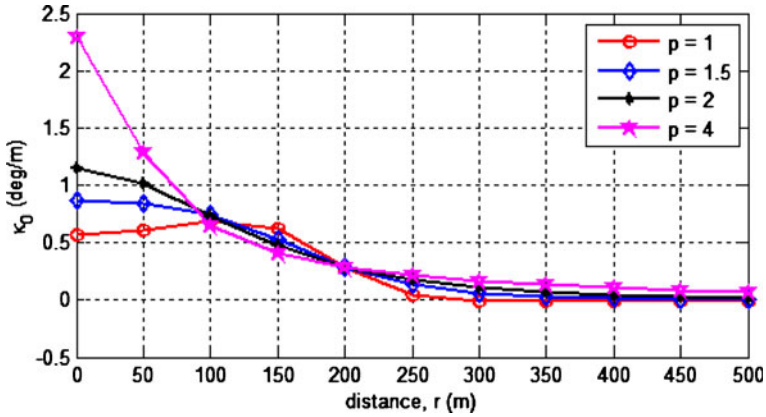

Fig. 3 A curvature of the vector field with regard to p when r_d is 200 m

too complicated or impossible. However, this is not a problem when this algorithm is loaded even in low-cost UAs, since the result can be calculated easily and fast using a numerical integration method. Now, length of the remaining flight path, l_{ren}, can be estimated using t_{eta} and s_c. When s_c is constant, then

$$l_{\text{ren}} = s_c \cdot t_{\text{eta}}. \tag{10}$$

And if t_{ren} is given, then the desired constant speed to arrive at the desired time can be derived as

$$s_r = \frac{l_{\text{ren}}}{t_{\text{ren}}} \tag{11}$$

Similarly, we can estimate and control the arrival position. The relationship between r and θ can be derived from Eq. 3 using the chain rule. In other words, we already know the derivative of the radial position and the angular position with respect to time; hence the angular position with respect to the radial position can be derived after a few integrations.

$$\frac{d\theta}{dr} = \frac{d\theta}{dt} d \frac{dt}{dr} = -\frac{p \cdot r_d}{r^2 - r_d^2} \tag{12}$$

Therefore,

$$\int_{\theta_c}^{\theta_f} d\theta = \int_{r_c}^{r_f} -\frac{p \cdot r_d}{r^2 - r_d^2} dr$$

$$\theta_f - \theta_c = -\frac{1}{2} p \cdot \left\{ g\left(r_f, r_d\right) - g\left(r_c, r_d\right) \right\} \tag{13}$$

where θ_c and θ_f are the current and desired final angular position, and

$$g\left(r_1, r_2\right) = \ln\left(r_1 - r_2\right) - \ln\left(r_1 + r_2\right). \tag{14}$$

Now, we can determine p if the desired position is given and the vehicle follows the speed and course command perfectly.

$$p = \frac{-2\left(\theta_f - \theta_c\right)}{g\left(r_f, r_d\right) - g\left(r_c, r_d\right)} \tag{15}$$

Notice that the difference between two the angular positions in Eq. 15 is not wrapped. If it is larger than 2π, then the vehicle will arrive at the point after turning around the target. The guidance parameter p is computed at every time step; therefore, tracking error will be compensated for.

Using Eqs. 11 and 15, UAs arrive at the desired position and time, i.e., they have the capability to capture a target simultaneously from all sides after t_{ren}. However, an UA has a constraint on air speed in case of a fixed-wing aircraft as

$$v_a = \{v_a \in \Re | 0 < v_{\text{stall}} < v_{\text{min}} < v_a < v_{\text{max}}\} \tag{16}$$

where v_{stall} is the stall speed, and v_{min} and v_{max} are the minimum and maximum available speed, respectively. Hence, they must reach a consensus on t_{ren} and each final position. The optimal and a stable method will not be handled in this paper; however, we propose a simple method. If some UA cannot arrive at the desired position after t_{ren}, the time of arrival is increased until all the UAs can arrive. On the other hand, if the desired position is very close to the UAs, then the computed

required speed can be slower than $v_{\min}$ in some scenarios. To compensate for this situation, the UA changes its direction of flight to the opposite direction and flies in order to increase the length of the flight path until the required speed becomes larger than $v_{\min}$. However, though effective enough, this method is not globally stable.

3.2 Control of Relative Spacing

It is important to control the relative spacing among multiple UAs. When the target is moving and we don't know where it will go, regular spacing is the best solution, since this formation might reduce the probability of losing the line-of-sight. It is also well known that if measurements from bearing sensors become perpendicular, the performance of the localization filter is maximized when two UAs are involved in a target localization mission [20]. Therefore this subsection will introduce how to control the relative spacing.

Ideas introduced in the previous subsection are for guidance from a far position to a close position. After arrival at the desired position, a different strategy is required to maintain the regular relative spacing. Frew et al. proposed a speed controller, and Yoon et al. proposed a heading change rate controller for the same purpose [12, 18]. In this subsection, we introduce a new idea based on the transfiguration of the vector field with variable r_d. The fundamental concept is very simple. If the vehicle must decrease the speed of the angular velocity, then increase r_d and decrease speed. On the other hand, if the vehicle must increase the speed of the angular velocity, then decrease r_d and increase speed. For this, variables of the vector field are defined to control the relative spacing $\Delta\theta$ where $\Delta\theta$ is $< \theta_n - \theta_{n-1} >$.

$$
\begin{aligned}
r_{dn} &= r_0 + K_r \langle \theta_n - \theta_{n-1} - \theta_{dn} \rangle \\
s_{rn} &= s_0 - K_s \left(r_{dn} / r_1 \right)^2 \langle \theta_n - \theta_{n-1} - \theta_d \rangle \, r_{dn}
\end{aligned} \tag{17}
$$

where r_0 is the reference standoff distance from the target, θ_{dn} is the desired relative spacing, K_r and K_s are the positive proportional gains, and s_0 is the reference speed. r_0, and s_0 are constant. The subscript n denotes the identification number of each vehicle. The speed controller was proposed by Frew et al. [12], and we supplement the standoff distance controller to improve performance. When these controllers are used simultaneously, the relative spacing error $< \Delta\theta - \theta_{dn} >$ converges to zero faster. By supplementing the standoff distance controller, we can make the variations of the speed command smaller. Before proving stability, we assume that the time constants of the system, τ_s and τ_χ, are not large, and the courses are almost aligned with tangents of the loitering circle. Hence, r_n and the $\dot{\theta}_n$ are approximately equal to r_{dn} and s_{rn}/r_{dn}, respectively. A new Lyapunov function is defined as

$$
\mathrm{V}_{r\theta} = \frac{1}{2} (r_n - r_{dr})^2 + \frac{1}{2} (\theta_n - \theta_{n-1} - \theta_d)^2 . \tag{18}
$$

And the time derivative of this function is

$$
\frac{\mathrm{d}V_{r\theta}}{\mathrm{d}t} = (r_n - r_{dr}) \dot{r}_n + (\theta_n - \theta_{n-1} - \theta_d) \left(\dot{\theta}_n - \dot{\theta}_{n-1} \right) \tag{19}
$$

where $\dot{r}_n = K_r \langle \dot{\theta}_n - \dot{\theta}_{n-1} \rangle$, $\dot{\theta}_n = s_{rn} / r_{dn}$, and $\dot{\theta}_{n-1} = s_{rn-1} / r_{dn-1}$ by the assumptions. Therefore,

$$
\frac{\mathrm{d}V_{r\theta}}{\mathrm{d}t} = (1 + K_r) (f_1 + f_2) \tag{20}
$$

where

$$
\begin{aligned}
f_1 &= -\frac{K_s \{r_r + K_r \cdot \theta_s\}^2 \theta_s^2}{r_n^2} - \frac{K_s \{r_r + K_r \cdot \theta_s\}^2 \theta_s^2}{r_{n-1}^2} \\
f_2 &= \frac{\theta_s \cdot s_0}{r_r + K_r \cdot \theta_s} - \frac{\theta_s \cdot s_0}{r_r - K_r \cdot \theta_s} \\
\theta_s &= \theta_n - \theta_{n-1} - \theta_d .
\end{aligned} \tag{21}
$$

$(1 + K_r)$ is always positive, and f_1 is less than or equal to zero. If $\theta_s > 0$, then the left term of the right hand side of f_2 is less than the right term, and f_2 becomes negative. On the other hand, if $\theta_s < 0$, the right term of the right hand side of f_2 becomes positive, however the magnitude is less than the left term; therefore, f_2 also becomes negative. When θ_s is zero, then Eq. 20 becomes zero, i.e., it is negative semi-definite.

3.3 Guidance Commands for Target Tracking

As mentioned before, the guidance commands are the ground speed and course command.

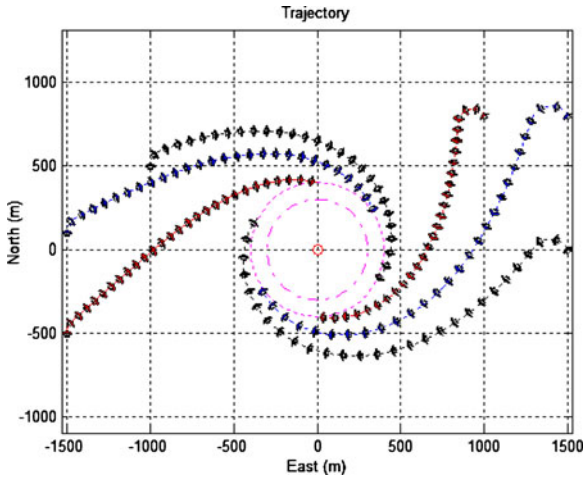

Fig. 4 Simulation #1. Trajectories to capture a target simultaneously when a target is stationary. $r_d = 300$ m, $r_f = 400$ m, and $t_f = 110$ s

Equation 3 is converted to Cartesian coordinates as

$$\begin{bmatrix} \dot{x}_r \\ \dot{y}_r \end{bmatrix} = \frac{-s_r}{\sqrt{r^4 + \left(p^2 - 2\right) r_d^2 \cdot r^2 + r_d^4}} \times \begin{bmatrix} \dfrac{r^2 - r_d^2}{r} x_r + p \cdot r_d \cdot y_r \\ \dfrac{r^2 - r_d^2}{r} y_r - p \cdot r_d \cdot x_r \end{bmatrix} \tag{22}$$

and it is used to generate the speed and course command.

We separated the guidance mode into two modes. The one is the capturing mode, and the other one is the loitering mode. Equations 11 and 15 are used for the capturing mode, and Eq. 17 is used for the loitering mode. In the capturing mode, estimated position of target after t_{ren} is fixed; therefore the commands are defined as

$$\begin{aligned} s_d &= s_r \\ \chi_d &= \operatorname{atan2}\left(\dot{y}_r, \dot{x}_r\right) \end{aligned} \tag{23}$$

In this mode, the relative position is computed with regard to the position of the target after t_{ren}.

Similarly, in the loitering mode, the commands are defined as

$$\begin{aligned} s_d &= s_r \\ \chi_d &= \operatorname{atan2}\left(\dot{y}_r + \dot{y}_t, \dot{x}_r + \dot{y}_t\right) \end{aligned} \tag{24}$$

The course command considers the motion of target to maintain regular standoff distance from a target. However, the motion is not considered at the speed command to eliminate the oscillated speed command. Therefore, the relative angular position changes irregularly, and this symptom is overcome by the relative spacing control. All

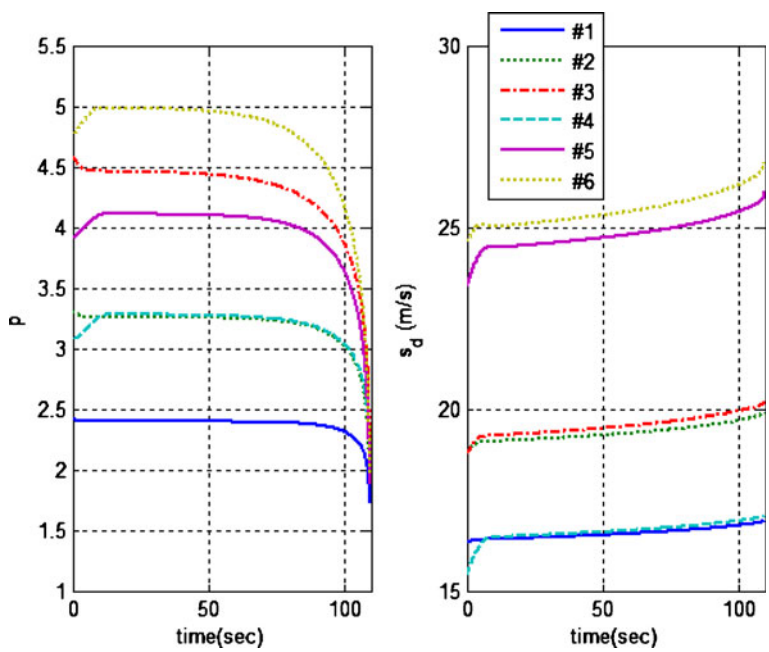

Fig. 5 Simulation #1. Guidance parameter p, and speed command s_d

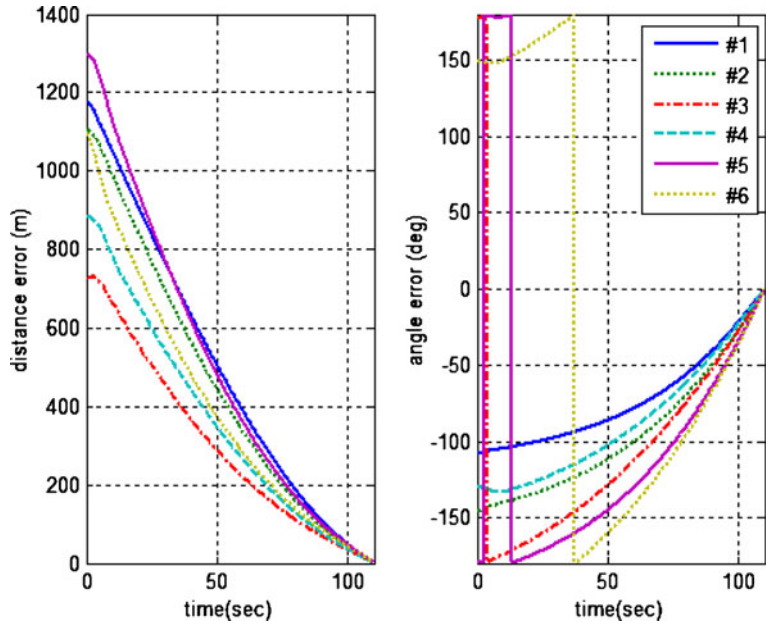

Fig. 6 Simulation #1. Radial and angular position error

these commands can be extended to n UAs, and the results will be presented in the next section.

4 Simulations

The basis of the modified vector field for standoff target tracking was proposed in Section 3. In this section, performance and characteristics will be analyzed through various simulation case studies. Notice that guidance commands in the following simulations are the ground speed and course. A kinematic model of all simulations is depicted in Eq. 2 where $v_{\min}$ is 15 m/s, $v_{\max}$ is 30 m/s, the maximum acceleration and deceleration are 2 m/s^2 and -1 m/s^2, respectively, and the maximum turning rate is 0.2 rad/s. Time constants τ_s and τ_χ are -2. We assume that there is no strong wind, and therefore, the commands from control layer can be tracked well; consequently, the dynamics is very similar to the kinematics of Eq. 2.

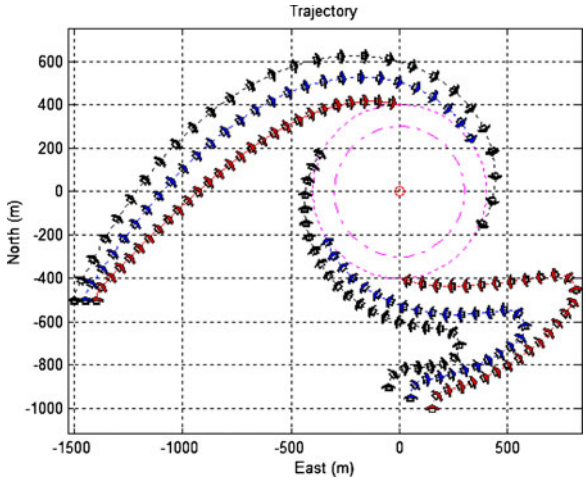

Fig. 7 Simulation #2. Trajectories to capture a target simultaneously when a target is stationary. $r_d = 300$ m, $r_f = 400$ m, and initial $t_f = 50$ s

4.1 Capturing Simultaneously from All Sides

When UAs are far from a target, surveillance or localization results are not good; therefore, in the capturing mode, the guidance layer just considers where they are after t_{ren}. The arrival position and time are controlled using Eqs. 11 and 15. The first simulation is done for the stationary target. r_d is 300 m and r_f is 400 m, $\theta_{d1}, \theta_{d2}, \theta_{d3}, \theta_{d4}, \theta_{d5}$, and θ_{d6} are 0 deg, 60 deg, 120 deg, 180 deg, 240 deg, and 300 deg, respectively, and t_{ren} is 110 s. Trajectories and commands are shown in Figs. 4 and 5, respectively. As you can see in Fig. 6, the UAs arrive at the desired position simultaneously from all sides;

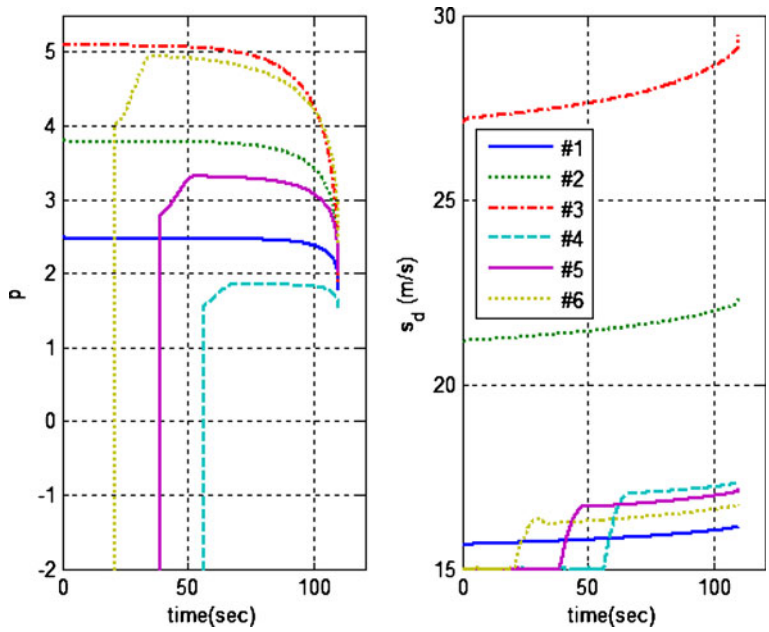

Fig. 8 Simulation #2. Guidance parameter p, and s_d

however, s_d and p are updated to reduce guidance error. Decreasing p increases the attraction force to a loitering circle, and increasing s_d implies that the ideal planned positions are located in front of the UAs.

Trajectories, commands, and errors of the second simulation are shown in Fig. 7, 8 and 9. In the second simulation, the initial desired time of arrival, t_{ren}, is 50 s, and UA #1, #2, and #3 are too far from the target; therefore they cannot arrive until the initial t_{ren}. Hence, the time of arrival is increased and becomes 110 s consensually. On the other hand, UA #4, #5, and #6 are too close due to increased t_{ren}. Hence, they fly in the opposite

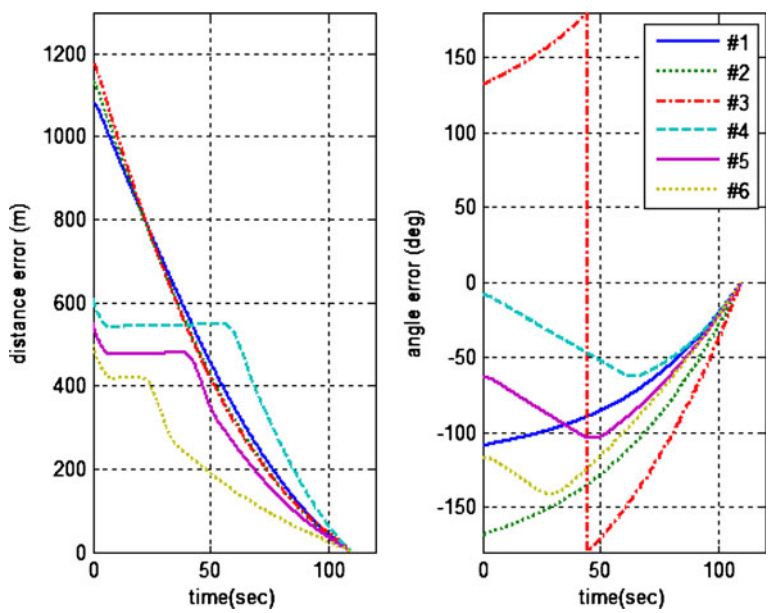

Fig. 9 Simulation #2. Radial and angular position error

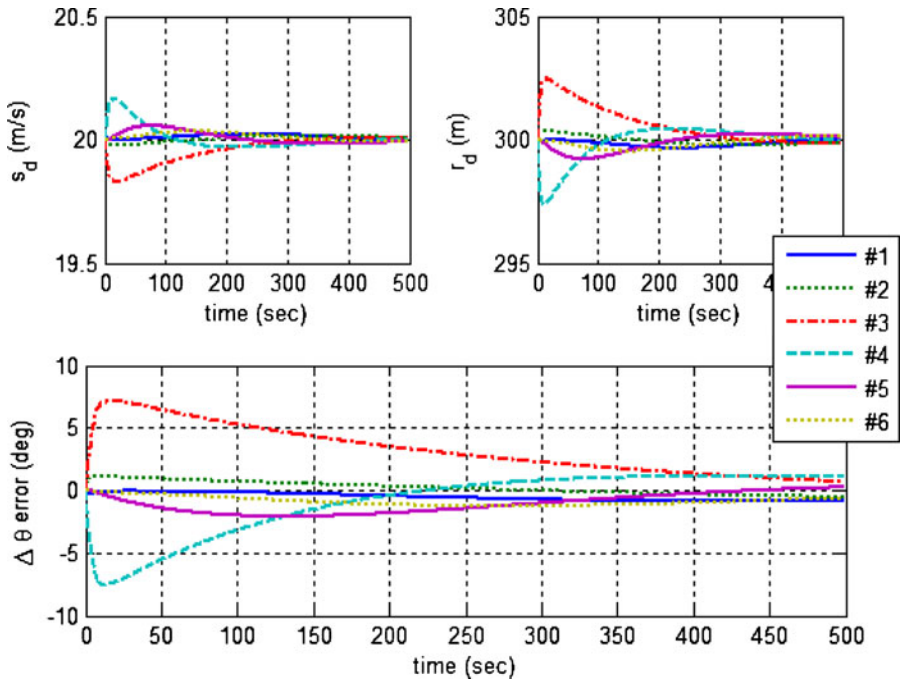

Fig. 10 Simulation #3. Speed commands and standoff distance commands of the third simulation when the loitering mode is engaged after capturing

direction in order to increase the length of the flight path. In this case, guidance commands force them to stop approaching the target via the maximum magnitude of p and the minimum s_d, and this receding maneuver continues until the computed s_r is in the region of Eq. 16. This is a useful and intuitive strategy even though its stability cannot be guaranteed.

4.2 Keeping Surveillance with Regular Spacing

After capturing the target simultaneously, the desired spacing among the UAs must be maintained regularly. When they capture the target, the speed of each UA is different and the courses are not aligned with their tangents of the loitering circle; therefore, just applying the vector field of Eq. 3 cannot maintain regular spacing, and consequently, the controller of Eq. 17 is required. The initial states of the third simulation are the same as the final states of the second simulation of Fig. 7, and the results are shown in Fig. 10. In the simulation, guidance parameter p is 1, s_0 is 20 m/s, K_r is 20, and K_s is 0.005. As you can see, the controller generates different speed and standoff distance commands to maintain regular spacing. The rate of convergence does not seem fast, since errors are not large. Large proportional gains make fast convergence and small steady state errors; however, it can bring unstable results due to time-delay of systems. As mentioned before, the initial states are not ideal; therefore, $\Delta\theta$ are increased at the start even though they are the same as the desired values.

In the fourth simulation, circumstances of rough initial states are assumed as you can see in Table 1, and the other conditions, such as control gains, are equal. Figure 11 shows the guidance commands and results of angular spacing. The angular spacing is converged to the desired value even though rough initial conditions are given. Figure 12 shows the results of a comparison

Table 1 Initial states of each UA for the fourth and fifth simulations

	#1	#2	#3	#4	#5	#6
r (m)	450	350	400	380	340	415
θ (deg)	0	70	100	180	240	290
s (m/s)	16	22	29	17.5	17	16.5
χ (deg)	107	165	−135	−69	−15	41

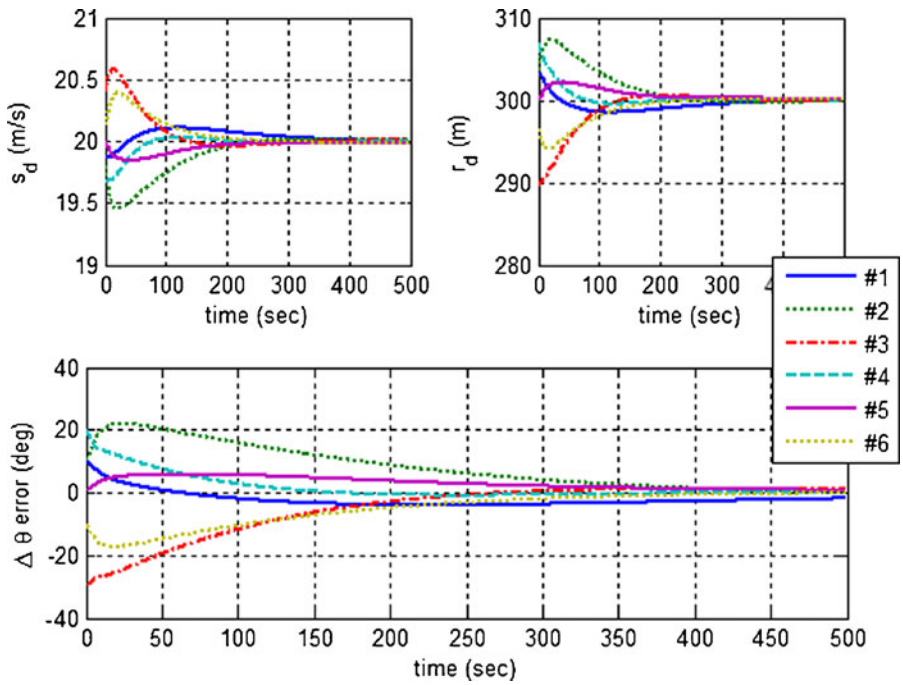

Fig. 11 Simulation #4. Speed commands and standoff distance commands with rough initial states

between Frew et al.'s controller and the proposed controller of Eq. 17. Angular spacing is converged to the desired value faster when the proposed controller is used. In case of UA #3, the commanded standoff distance is less than r_d; therefore, the angular velocity is increased faster than with the

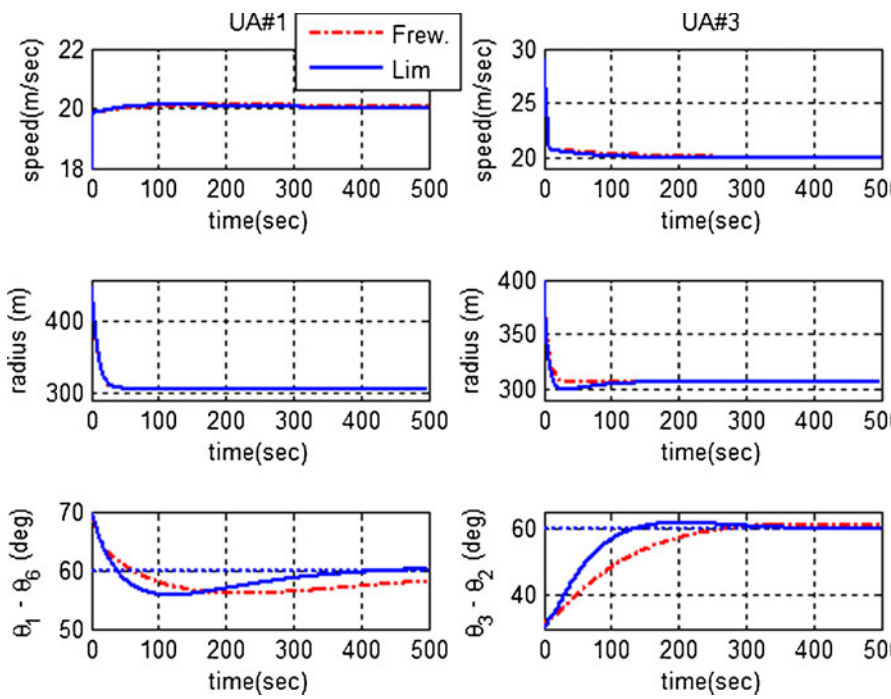

Fig. 12 Simulation #4. States of UA #1 and #3. *Red dotted lines* are states with Frew et al.'s controller, and *blue lines* are states with the proposed controller

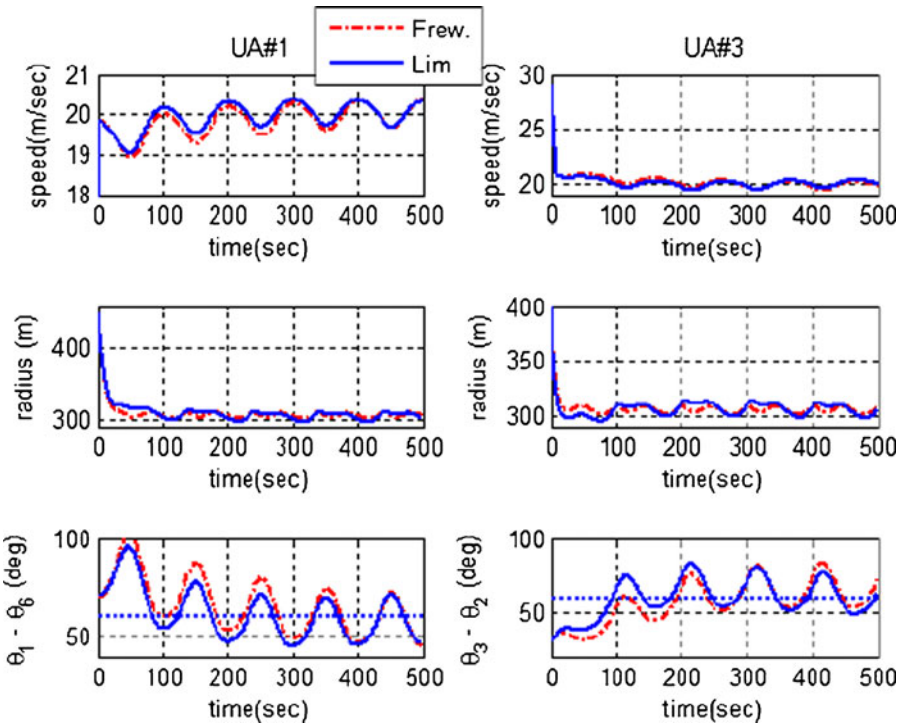

Fig. 13 Simulation #5. States of UA #1 and #3. *Red dotted lines* are states with Frew et al.'s controller, and *blue lines* are states with the proposed controller

previous controller. Detailed states of the other UAs are omitted for lack of space.

When a target is moved, the desired ground speed and course command can be obtained by adding the velocity of the target to the velocity command of the UAs. However, if the target moves fast, then the ground speed command can exceed Eq. 16, and an oscillated speed command with much variation might be not efficient when UAs are operating, since it can bring a little undesired torque change to an aircraft body, and the time constant of the electric motor is not small. Therefore, from the point of view of operations, a ground speed command with less variation is fascinating. Consequently, the speed command is not compensated for as you can see in Eqs. 23 and 24.

The fifth simulation is done with the moving target which moves at a speed of 5 m/s. All other initial states and control gains are the

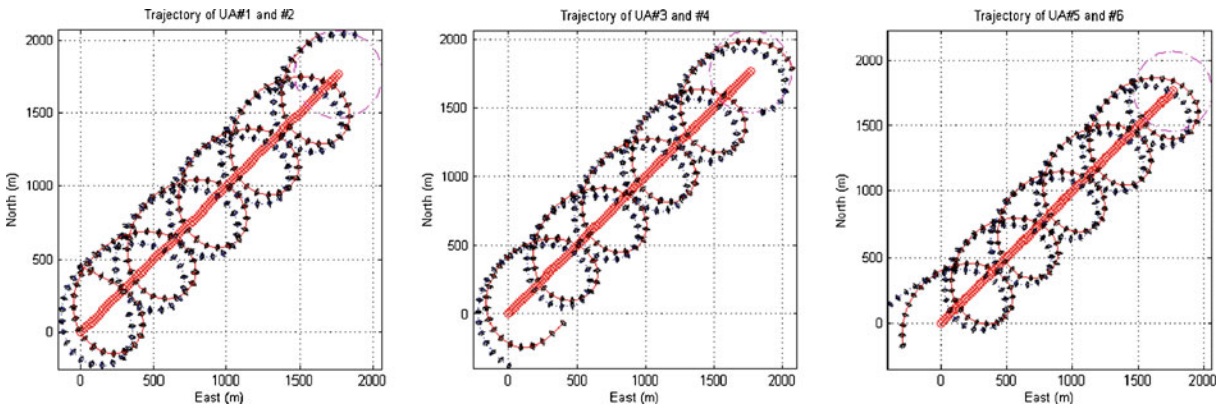

Fig. 14 Simulation #5. Tracking trajectories of UAs when target moves at a speed of 5 m/s

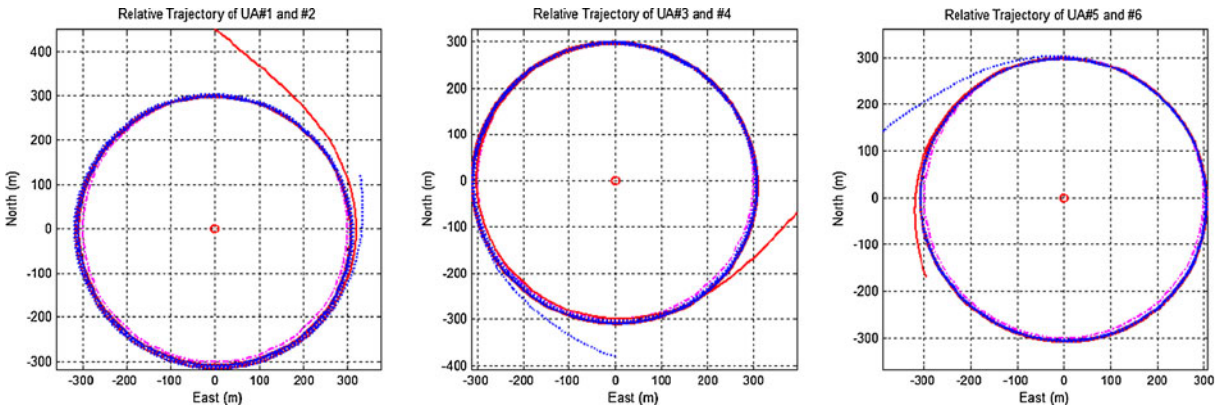

Fig. 15 Simulation #5. Relative trajectories of UAs from a moving target

same as in the fourth simulation. The states are shown in Fig. 13. The proposed controller shows a faster convergence. The trajectories are shown in Figs. 14 and 15.

5 Conclusion and Future Works

The topic of this paper is target tracking strategies for a team of UAs. The vector field is applied to solve this problem with the basic approach as Frew et al. has already described it [12]. We have extended our investigation to improve tracking performance. Our first achievement is the strategy to capture a target simultaneously from all sides by the modified vector field. The vector field is modified so that UAs are guided to satisfy constraints of arrival positions by a suitable guidance parameter p which is determined very simply based on current and terminal goal positions. This value is updated every time step to eliminate error. After deriving p, a path and its length are estimated using a numerical integration method, so the time of arrival can be satisfied by a suitable speed command. Simulation results show that UAs can capture a target when they track guidance commands properly.

The second achievement is improving the performance of maintaining the regular spacing among the UAs. Frew et al. proposed a speed controller to maintain the desired spacing and guaranteed the minimum standoff distance from the target [12]. We assume that a slightly smaller distance is allowed; therefore, the standoff distance controller is supplemented to increase or decrease the angular velocity. Simulation results show that the proposed hybrid controller reduces error faster than Frew et al.'s controller.

None of the simulation results, including those in Frew et al.'s paper, consider a fast moving target. If a target moves fast, then loitering around the target might be impossible or inefficient. In this case, following with a sinusoidal path is a better approach, and vector field guidance for this case is our future work. Another future work is designing the control layer to track the commands from the guidance layer, even though there are disturbances such as wind.

References

1. Kaminer, I., Pascoal, A., Hallberg, E., Silvestre, C.: Trajectory tracking for autonomous vehicles: an integrated approach to guidance and control. J. Guid. Control Dyn. **21**, 29–38 (1998)
2. Aguiar, A.P., Hespanha, J.P., Kokotovic, P.V.: Path-following for nonminimum phase systems removes performance limitations. IEEE Trans. Automat. Contr. **50**, 234–239 (2005)
3. Khatib, O.: Real-time obstacle avoidance for manipulators and mobile robots. In: IEEE International Conference on Robotics and Automation, 1985. Proceedings, pp. 500–505 (1985)
4. Borenstein, J., Koren, Y.: Real-time obstacle avoidance for fact mobile robots. IEEE Trans. Syst. Man Cybern. **19**, 1179–1187 (1989)
5. Meenakshisundaram, V., Gundappa, V., Kanth, B.S.: Vector field guidance for path following of MAVs in three dimensions for variable altitude maneuvers.

International Journal of Micro Air Vehicles **2**, 255–265 (2010)
6. Koren, Y., Borenstein, J.: Potential field methods and their inherent limitations for mobile robot navigation. In: IEEE International Conference on Robotics and Automation, 1991. Proceedings, vol. 2, pp. 1398–1404 (1991)
7. Koditschek, D.: Exact robot navigation by means of potential functions: some topological considerations. In: IEEE International Conference on Robotics and Automation, 1987. Proceedings, pp. 1–6 (1987)
8. Spry, S.C., Girard, A.R., Hedrick, J.K.: Convoy protection using multiple unmanned aerial vehicles: organization and coordination. Am Control Conf **5**, 3524–3529 (2005)
9. Rysdyk, R.: Unmanned aerial vehicle path following for target observation in wind. J. Guid. Control. Dyn. **29**, 1092–1100 (2006)
10. Waydo, S., Murray, R.M.: Vehicle motion planning using stream functions. Robotics and Automation, 2003. In: IEEE International Conference on ICRA '03, Proceedings, vol. 2, pp. 2484–2491 (2003)
11. Rimon, E., Koditschek, D.E.: Exact robot navigation using artificial potential functions. IEEE Trans. Robot. Autom. **8**, 501–518 (1992)
12. Frew, E.W., Lawrence, D.A., Morris, S.: Coordinated standoff tracking of moving targets using lyapunov guidance vector fields. J. Guid. Control. Dyn. **31**, 17 (2008)
13. Lawrence, D.A., Frew, E.W., Pisano, W.J.: Lyapunov vector fields for autonomous unmanned aircraft flight control. J. Guid. Control. Dyn. **31**, 10 (2008)
14. Griffiths, S.R.: Remote terrain navigation for unmanned aerial vehicles. Master, Department of Mechanical Engineering, Brigham Young University (2006)
15. Nelson, D.R., Barber, D.B., McLain, T.W., Beard, R.W.: Vector field path following for miniature air vehicles. IEEE Trans. Robot. **23**, 519–529 (2007)
16. Elston, J., Frew, E.: Net-centric cooperative tracking of moving targets. Presented at the AIAA Infotech@Aerospace Conference and Exhibit, Rohnert Park, California (2007)
17. Zhu, S., Wang, D., Chen, Q.: Standoff tracking control of moving target in unknown wind. Presented at the IEEE Conference on Decision and Control, Shanghai, People's Republic of China (2009)
18. Yoon, S., Kim, Y.: Cooperative control of multiple unmanned aircraft for standoff tracking of a moving target. Journal of the Korean Society for Aeronautical and Space Sciences **39**, 114–120 (2011)
19. Zhu, S., Wang, D.: Adversarial ground target tracking using UAVs with input constraints. J. Intell. Robot. Syst. **65**, 521–532 (2012)
20. Lee, W., Bang, H., Leeghim, H.: A cooperative guidance law for target estimation by multiple unmanned aerial vehicles. Proc. Inst. Mech. Eng., G J. aerosp. eng. **225**, 1322–1335 (2011)